Microspectrophotometry of Single Rhabdoms in the Retina of the Honeybee Drone (*Apis mellifera* ♂)

R. B. MURI* and G. J. JONES

From the Département de Physiologie, Centre Médical Universitaire, CH-1211 Genève 4, Switzerland

ABSTRACT The relative absorption spectra of the bistable photopigment of single rhabdoms from the dorsal region of the retina of the honeybee drone were obtained using slices of retina fixed in glutaraldehyde; less accurate measurements on unfixed tissue gave difference spectra that were similar to those for fixed retinae. The method used was based on measurements of absorbance changes during saturating adaptations of the visual pigment to different monochromatic lights. It is similar to previous methods based on measurements of difference spectra amplitudes, but is simpler to use and more accurate. The predominant pigment has states that absorb maximally at 446 (rhodopsin) and 505 nm (metarhodopsin). In addition, there is a small amount of another pigment whose two states absorb maximally at ~340 (UV) and 460 nm.

INTRODUCTION

There is evidence that the photopigments in many invertebrate photoreceptors have two thermostable forms or states that are photointerconvertible (see reviews by Goldsmith, 1972; Hamdorf, 1979). Absorption of photons by the state called rhodopsin is primarily responsible for the generation of the receptor potential (Hamdorf et al., 1968); however, absorption of photons by the other state, metarhodopsin, can also affect the membrane potential, notably when the membrane has previously been depolarized by a massive conversion of rhodopsin to metarhodopsin (Hochstein et al., 1973). An investigation of the relative contributions of rhodopsin and metarhodopsin to the electrical responses of the photoreceptor cells requires an accurate knowledge of the absorption spectra of the two states. The aim of the present work was to determine the absorption spectra of the photopigments in the dorsal region of the retina of the honeybee drone, a tissue that has been the object of several electrophysiological studies (for a review of the earlier work, see Baumann, 1975).

* Died tragically in a hang-gliding accident, September 13, 1982.

Address reprint requests to Dr. G. J. Jones, Dépt. de Pharmacologie, Centre Médical Universitaire, CH-1211 Genève 4, Switzerland.

J. GEN. PHYSIOL. © The Rockefeller University Press · 0022-1295/83/10/0469/28 $1.00

Volume 82 October 1983 469–496

The absorption of light by an invertebrate rhodopsin results in the formation of another stable pigment with an overlapping absorption spectrum. Thus, the absorption spectra of the two pigment states cannot generally be obtained directly from a difference spectrum, i.e., by comparing the absorption before and after illumination, as can usually be done for the α peak of vertebrate photopigments, which bleach after illumination. A method for determining the relative absorption spectra of a bistable photopigment was introduced and developed by Stavenga (1975*a*, 1976). The method was based on a comparison of the relative amplitudes of the difference spectra obtained after saturating adaptation of the photopigment with different wavelengths of monochromatic light. The photoequilibrium spectrum (Stavenga, 1975*a*; Hillman, 1979) obtained from these amplitudes is a measure of the fraction of the pigment in each state after the saturating adaptations, and can be combined with the difference spectrum to obtain the relative absorption spectra. However, the resulting absorption spectra are often subject to considerable experimental error (Stavenga, 1976), principally because of the difficulty of accurately measuring difference spectra amplitudes when the adapting light converts only a small fraction of the pigment from one state to the other.

In the present paper, an extension of the method of Stavenga (1975*a*) is described in which only the maximum value of the photoequilibrium spectrum is used in the calculation of the relative absorption spectra. A new spectrum is introduced: the conversion spectrum. This spectrum measures the optical density change during adaptation at different wavelengths, after an initial saturating adaptation at the wavelengths that convert the maximum amount of pigment to one or the other stable state. It is shown that the combination of either of the two conversion spectra with the difference spectrum, together with the maximum amplitude of the photoequilibrium spectrum, enables the relative absorption spectra of the two stable states of the photopigment to be calculated. The advantage of the present method is that all these measurements are made after a large fraction of the pigment has been converted to one state or the other, and the resulting spectra can be expected to have a smaller experimental error than previous methods. In this work, the method has been used to determine the absorption spectra of the photopigment in the honeybee drone, but it is applicable, in principle, to any bistable pigment.

In the drone retina, each ommatidium contains six large electrically coupled photoreceptor cells that share a fused rhabdom (Perrelet, 1970; Shaw, 1969). Spectral sensitivity curves have been determined from measurements of intracellularly recorded receptor potentials (Autrum and Zwehl, 1964; Bertrand et al., 1979). All the cells recorded from by our laboratory to date in the dorsal region of the retina have been found to have their maximum sensitivity at the same wavelength (450 nm). This is indistinguishable from the wavelength of maximum absorbance of one of the two major pigment states measured by microspectrophotometry in the present work, which is therefore defined as rhodopsin, whereas the state with maximum absorbance at a longer wavelength (505 nm) is metarhodopsin.

Each ommatidium of the drone retina also contains three small photoreceptor cells that contribute far fewer microvilli to the rhabdom than do the six large ones (Perrelet and Baumann, 1969). It would not be surprising, therefore, if the rhabdom contained small amounts of a photopigment different from the predominant one. Evidence will be presented for the existence of a small amount of a second photopigment that absorbs in the ultraviolet.

METHODS

Preparation

Drones were obtained locally in the summer from Ms. E. Coe, Tucson, AZ, or from Mr. Merin Nathan, Chicoun Amal, Hadera, Israel, during the winter. Before the experiment the drones were kept in darkness at 30°C with workers that were fed with sugar solution. The heads of the drones were severed in room light and, for most experiments, were fixed by immersion for 3 h in 2.5% glutaraldehyde solution (phosphate buffer, 100 mM, pH 7.4; temperature 18–20°C). A tangential cut was made through the dorsal part of the eye in such a way as to remove the dioptric apparatus (cornea and crystalline cone) and the main part of the screening pigment from an area of the retina. A second cut, parallel to the first, was made superficial to the basement membrane to produce a slice between 100 and 200 μm thick with some ommatidia in its center perpendicular to the two parallel surfaces. The slice was placed on a quartz microscope coverslip and surrounded by a thin ring of vaseline grease. A drop of insect Ringer was added and a second quartz coverslip was placed over the whole. The grease ring seal prevented evaporation and served as a spacer that prevented the specimen from being crushed. The bathing solution was insect Ringer with the following composition: 287 mM NaCl; 3.1 mM KCl; 1.8 mM $CaCl_2$; 10 mM Tris (Bader et al., 1976). The pH was adjusted to 7.4 with HCl. The preparation, between the coverslips, was placed between condenser and objective of the microspectrophotometer without the use of immersion fluid.

The Microspectrophotometer

A double-beam microspectrophotometer has been constructed that permits measurements extending into the ultraviolet (UV), and is equipped with a third beam that can be used to change the pigment states. The optical arrangement is outlined in Fig. 1; a detailed description is given in Muri (1979). The source is a xenon high-pressure lamp (XBO 1600; Osram GmbH, Munich, Federal Republic of Germany [FRG]) with a power supply stabilized to 0.5%.

The arc is projected by mirror optics onto the entrance slit of an MM12G dual grating monochromator (Carl Zeiss, Oberkochen, FRG) of 250 mm focal length. To reduce possible effects of arc wandering, the image of only a small part of the area of the plasma is admitted by the entrance slit: if the arc moves laterally by 10% of its width, the flux changes by <2%. Over the wavelength range of the monochromator (190–750 nm), the bandwidth for a given slit width is almost constant and the wavelength is linear with the rotation angle. Small deviations are automatically corrected for by computer (see Muri, 1979). The scanning speed can be varied between 60 and 0.06 nm/s. The small entrance aperture of the monochromator allows a spectral resolution of 0.5 nm. The monochromator scale was calibrated against a mercury emission lamp, and the calibration was stored in the computer memory. Intermediate wavelength positions are calculated by linear interpolation.

The monochromator exit slit is projected by means of mirror optics into the variable entrance diaphragm of the Zeiss Ultrafluar microscope condenser, with a maximum numerical aperture (NA) of 0.8. A field stop of variable size and shape, placed after the slit-condenser projection optics, is projected by the condenser into the specimen plane. With the condenser NA set at 0.4, the Airy disk in the specimen plane has a diameter of 1.0–1.5 μm at a wavelength of 550 nm. The specimen plane is projected by the microscope tube optics into an intermediate projection plane where the image

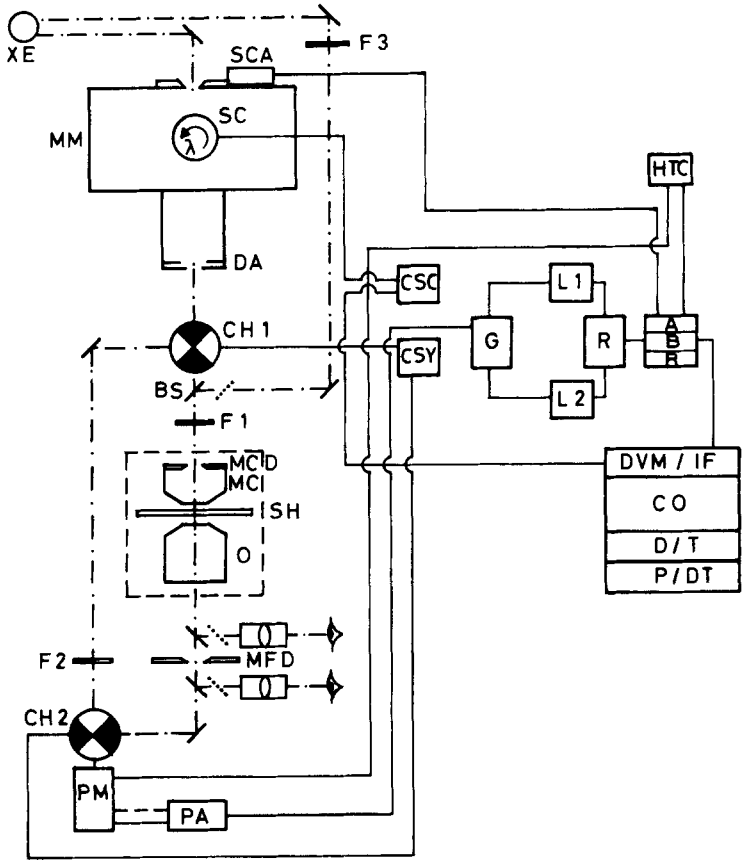

FIGURE 1. Schematic diagram of the microspectrophotometer. XE, Xenon light source; MM, monochromator; CH1, CH2, mirror wheels; BS, removable beam combiner; DA, MCD, MFD, diaphragms in the measuring beam; F1, F2, F3, light filters; MC, microscope condenser; O, objective; SH, sample holder; PM, photomultiplier; PA, preamplifier; G, gate; L1, L2, lock-in amplifiers; R, ratiometer with outputs A, B, or R = B/A (A: reference beam signal; B: measuring beam signal); HTC, high-tension supply for the PM (feedback controlled by channel A or constant); SCA, monochromator slit control (feedback controlled by channel A); SC, scanning motor; CSC, scanning control; CSY, mirror wheel synchronizer; DVM, AD converter; IF, interface to computer; CO, computer; D, T, magnetic disk and tape storage; P, D, printout, display.

areas not used for measuring are screened by a field stop of variable size and shape (usually rectangular).

The microscope objective used for most of the experiments described here was a Zeiss Ultrafluar 32 (NA 0.4). The only exceptions were the two experiments (illustrated in Figs. 3 and 4), in which the optimal NA for light entry into the rhabdom and the transmittance profile of the rhabdom were measured: for these two experiments an Ultrafluar 100 (NA 0.85) was used in order to capture as much of the light leaving the rhabdom as possible. In the other experiments the Ultrafluar 32 was considered sufficient, since only changes in absorption were measured, and this objective has a lower magnification, minimizing possible errors caused by the instability of the preparation. In addition, the experiment shown in Fig. 3 indicated that entry into the rhabdom hardly increased beyond NA >0.35, and thus little advantage can be expected with an objective of larger NA. Furthermore, in one experiment (see Muri, 1979) the light capture was measured using different objectives of different NA; the results indicated that light capture was not greatly improved for NA >0.4.

The intensity of the measuring beam can be varied by means of UV-grey filters (Carl Zeiss) and diaphragms over a range of six decades. Because the preparation filled the whole visual field of the objective, it was not possible to pass the reference beam through the same condenser as the measuring beam (see Muri, 1979). Instead, a mirror wheel, composed of two 90° segments placed after the field stop, deviates the beam alternately into a reference and a measuring beam axis. A dark period between the measuring and reference phases is obtained by fixing a black Maltese cross on the mirror wheel. Each reference, dark, and measuring period occupies one-eighth of the disk. The rate of chopping by the mirror is 12.8 Hz. This rate was chosen as a compromise between the vibrational limitations of the mirror motors and a minimum rate of chopping for a successful subsequent electronic amplification. A second rotating mirror wheel, synchronized with the first and placed after the field stop, directs the two beams alternately onto the cathode of a photomultiplier (9558 QB; Thorn EMI plc, Middlesex, England) that can be cooled to −20°C by a Peltier system. To avoid motion of the beam on the preparation, the first mirror wheel only deviates the reference beam. Because the optical pathlength of the reference beam is long, the accuracy of the mirror alignment must be very high (better than ±6′) to avoid geometric displacement of the beam on the photocathode, which is not very homogenous. All mirrors are coated with Alflex-UV (Balzers AG, Lichtenstein) coating with high spectral uniformity. The transmission optics is of fused quartz (Suprasil I; Heraens GmbH, Hanau, FRG) with high spectral uniformity from the infrared (IR) to the UV. The light flux is kept constant for all wavelengths by a feedback from the reference beam that controls the slit width. As a consequence, the bandwidth is not constant during a spectral scan, but it does not exceed 3 nm and is <1 nm between 350 and 500 nm. A high-tension feedback control of the photomultiplier was also installed in the instrument, but it was not used very often because of the considerable noise amplification when the high tension is increased.

A gate after the preamplifier separates the signals originating from the measuring (B) and the reference beam (A). A and B are amplified in lock-in amplifiers (Brower Laboratories, Inc., Newton, MA) whose outputs are matched to the entrance of a ratiometer system, which forms the ratio B/A (or A/B). Use of the ratio elminates perturbation parameters, such as emission lines of the radiation source, that are not fully compensated by the feedback, residual motion effects, and inhomogeneities of the instrument optics. As operated, the instrument measures transmittance. Measured values are digitized and stored by a 21 MX computer (Hewlett-Packard Co., Palo

Alto, CA), connected to the output of the ratiometer system. The computer calculates optical densities and difference spectra.

The illumination for positioning of the preparation and adaptation of the photopigment is by a third beam, which bypasses the monochromator. This beam is brought back to the optical axis of the measuring beam by a system of sliding mirrors, located behind the first chopper mirror. Intensity is varied by diaphragms, and the wavelength is varied by interference filters or an interference monochromator (Veril 200; Schott Glassworks, Mainz, FRG). For positioning the preparation, the Schott colored glass filter RG 720 is used. When the third beam is in use, the photomultiplier is protected by a shutter.

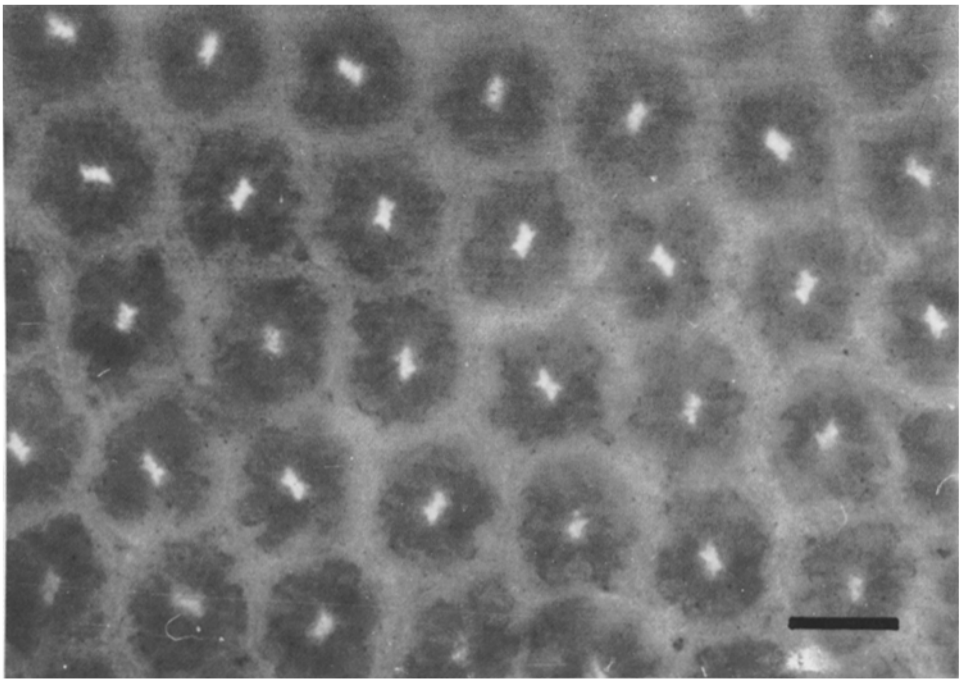

FIGURE 2. Microphotograph of a transilluminated slice of the honeybee drone retina. The slice is ~150 μm thick. The retinula cells and pigment cells appear darker than the parallelogram-shaped rhabdoms because of the light guide properties of the rhabdoms. To measure the spectral absorbance of single rhabdoms, the measuring beam was centered on one rhabdom and the surrounding area was blocked by a diaphragm in the first projection plane (MFD in Fig. 1). Calibration bar, 20 μm.

RESULTS

Scattering and Light Guide Properties of the Preparation

The light passing through the preparation is affected by scattering and light guide properties; the effect of the latter is illustrated in Fig. 2, which shows a transilluminated slice of retina fixed in glutaraldehyde, as observed through the microspectrophotometer objective. The field was uniformly illuminated

from below, but the rhabdoms appear brighter than the rest of the photoreceptor cells and the glial cells because the rhabdoms have light guide properties.

To measure changes in the absorbance of the photopigments, we wanted to pass as great a fraction as possible of the incident light into a single rhabdom. The greater the NA of the condenser, the greater is the precision with which the incident light can be focused on the end of rhabdom. However, since the rhabdom acts as a light guide, it accepts incident light

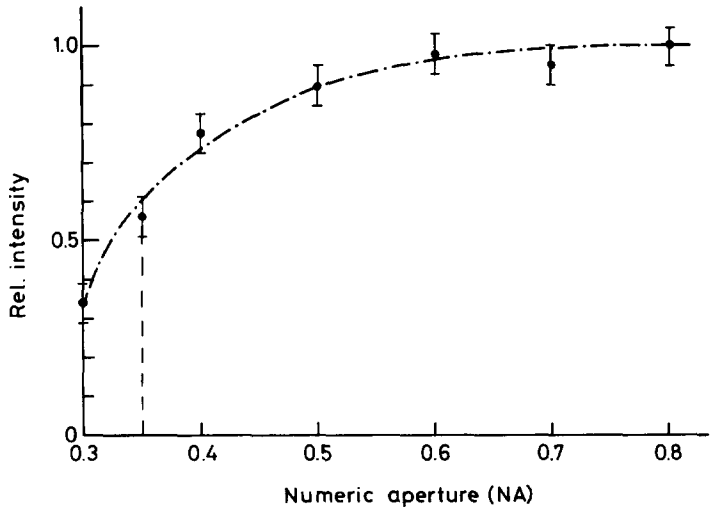

FIGURE 3. Relative light flux passing through a rhabdom as a function of the numerical aperture (NA) of the incident light beam. The Airy disk of the incident light beam on the lower plane of the retinal slice had a diameter of ~1.5 μm at 515 nm wavelength, and was smaller than the small side of the parallelogram-shaped rhabdom. The NA of the objective was 0.85. The microscope objective was focused on the lower cutting plane of the preparation. The preparation was moved outside the light beam and the microscope condenser was focused at the same level. The preparation was then centered on the light beam until a rhabdom was brightly illuminated (a maximal signal was obtained when the preparation was moved in the x and y directions). For an NA >0.35–0.4, the light flux through the rhabdom tends to saturate. Each point is the mean ± SEM from measurements of eight rhabdoms in different retinae.

only over a range of angles to its axis. Hence, measurements were made to find the optimum NA for the condenser and to estimate the acceptance angle of a rhabdom. A light spot so small that its diameter was determined almost entirely by diffraction effects (the Airy disk) was focused on the lower end of a rhabdom (see legend to Fig. 2) and the light leaving the upper end of the rhabdom was collected by an objective of NA 0.85 and measured. The transmitted light flux depended on the NA of the condenser; the relation is shown in Fig. 3.

If the preparation, at the focus of the condenser, was replaced by a diaphragm with the same shape as the rhabdom cross section, the light flux would increase at least with the square of the NA, because of the increasing half-angle of incident cone and also because of the decreasing diameter of the diffraction pattern. In contrast, when the light was focused on a rhabdom, for NA >0.35, the light flux tended to saturate. Therefore, in subsequent experiments, an NA of 0.35 was used, since it gave an optimal flux through the rhabdom. Taking into account the refractive index of the Ringer solution

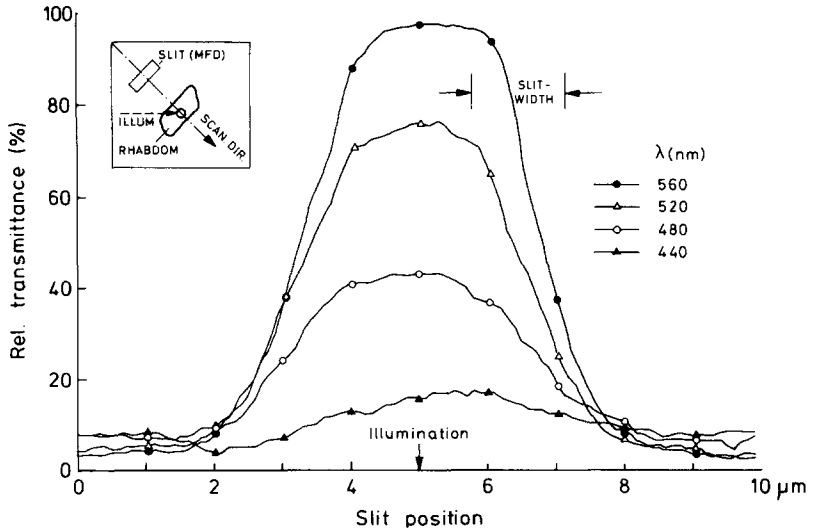

FIGURE 4. Transmittance profile of a transilluminated ommatidium. The length of the ommatidium was ~150 μm. The measuring beam (diameter of the Airy disk 1.5 μm) was placed in the center of the rhabdom. A slit 1.5 × 4 μm was moved over the image of the preparation at the field diaphragm level (MFD). The scanning direction was perpendicular to the long side of the rhabdom cross section. The NA of the incident beam was 0.4 and that of the objective was 0.85. The figure shows relative transmittance profiles at different wavelengths of the measuring beam. At short wavelengths, a strong decrease of the peak amplitude is accompanied by an increase of the extrarhabdomeric stray light level.

(1.34), an NA of 0.35 corresponds to an acceptance angle for the rhabdom of 15°. The angle of total reflection calculated with the refractive indices found by Varela and Wiitanen (1970) and corrected by Stavenga (1975*b*) is ~11°. The difference between the experimental and theoretical results is probably due to scattering inside the rhabdom.

Evidence for scattering from the rhabdom to the rest of the tissue is given in Fig. 4. The end of the rhabdom was illuminated with a small spot of light and the light emerging from the preparation was scanned in the plane of the field diaphragm (MFD in Fig. 1) by a slit corresponding to 1.5 × 4 μm in the

object plane. As the slit was moved across the image of the rhabdom, a pronounced peak in light intensity was recorded. Fig. 4 shows scans at four wavelengths. At shorter wavelengths less light emerged from the rhabdom and more was scattered into the surrounding space.

Transmittance Spectra

The transmittance spectrum of a rhabdom previously adapted to yellow-green light (538 nm) is shown as curve 1 in Fig. 5. Transmittance through the rhabdom decreases markedly at shorter wavelengths (note the increase in gain by a factor of 20 for wavelengths shorter than 450 nm). This decrease is due not only to absorption in the rhabdom but also to the light-scattering

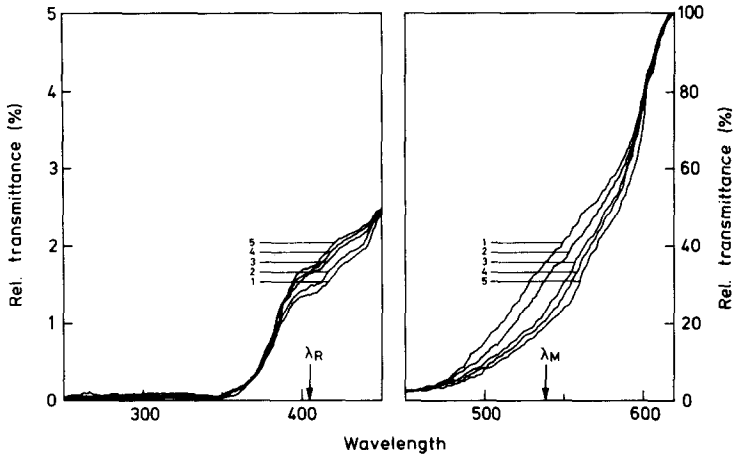

FIGURE 5. Spectral transmittance measured through a single rhabdom. Because the accessory absorbance increases strongly at short wavelengths, the sensitivity of the amplifier was increased by a factor of 20 at 450 nm to show better the absorbance change at short wavelengths. Curve 1 was obtained after exposure of the retina to bright light of 538 nm (λ_M) wavelength. Curves 2–5 were obtained after exposure to light of wavelength 405 nm (λ_R) and exposure times of 30 s, and 1, 2, and 3 min.

phenomenon described above (see Fig. 4). Also shown in Fig. 5 is the effect of violet (405 nm) illumination of the rhabdom for various times. Violet illumination increased the transmittance in the violet and decreased it in the green, and the relative change increased with the duration of the illumination.

Spectra such as those shown in Fig. 5 remained stable for hours if the preparation was kept in darkness. However, after bright illumination with yellow-green (538 nm) light, curve 1 could again be obtained. This stability and reversibility of the photopigment system is documented in Fig. 6. A rhabdom was first adapted with yellow-green light (538 nm), and the transmittance was measured at 528 nm. The measuring beam was of very weak intensity to avoid significant photoisomerization. The rhabdom was subsequently adapted with violet (405 nm) light, with yellow-green, and again with

violet light, over a short period of time. The transmittance at 528 nm is seen to change in a very reproducible way. After the second violet adaptation, the preparation was left in darkness and the transmittance at 528 nm was measured at intervals of 1, 2, 4, and 8 h. The slight increase in transmittance over the 8-h period can be attributed entirely to photoconversion by the measuring beam. Adaptation with yellow-green light after 8 h restored the control transmittance at 528 nm.

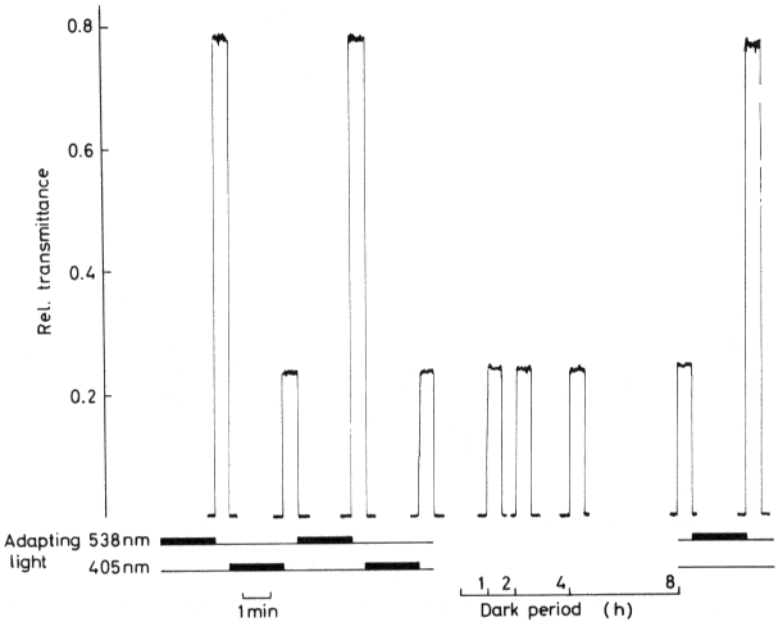

FIGURE 6. Stability and reversibility of the green-violet-absorbing pigment. The rhabdom was first adapted to green (538 nm) light, then to violet (405 nm), and once again to green light. After each adaptation the relative transmittance was measured at 528 nm. The rhabdom was again violet-adapted and kept in the dark. The transmittance at 528 nm was measured for 30 s periods after 1, 2, 4, and 8 h. Then the rhabdom was again green-adapted and the transmittance was measured. The transmittance is the same as that preceding the dark period, which showed that the preparation did not move during the dark period. The transmittance of the violet-adapted state remained almost constant during the dark period; the small increase can be entirely attributed to photoconversion by the measuring beam.

It was not possible to measure the stability of the pigment states in unfixed preparations because, as described in the next section, the signal-to-noise ratio was very small. Results from electrophysiological studies in the drone, however, suggest that the metarhodopsin is stable for at least 30 min (Bader et al., 1982).

Difference Spectra

From curves such as 1 and 5 in Fig. 5, difference spectra were calculated as the change in optical density of spectral scans after different adapting illu-

minations. Difference spectra obtained after conditioning at 405 nm and then illuminating for various times at 538 nm are shown in Fig. 7. The longest illumination time (curve *E*) produced the maximum possible absorbance change.

Such difference spectra were obtained in 40 rhabdoms from 15 drones. The wavelength of the long-wavelength peak was reproducible to within ±5 nm; there was more noise at short wavelengths, but the peak wavelength was always within ±8 nm of the mean. The ratio of the amplitudes of the two peaks was 3.8 ± 0.4 (mean ± SEM). There was an isosbestic point, which indicates that these manipulations converted a single photopigment between two stable states.

The first difference spectra were obtained from unfixed retinas. In the

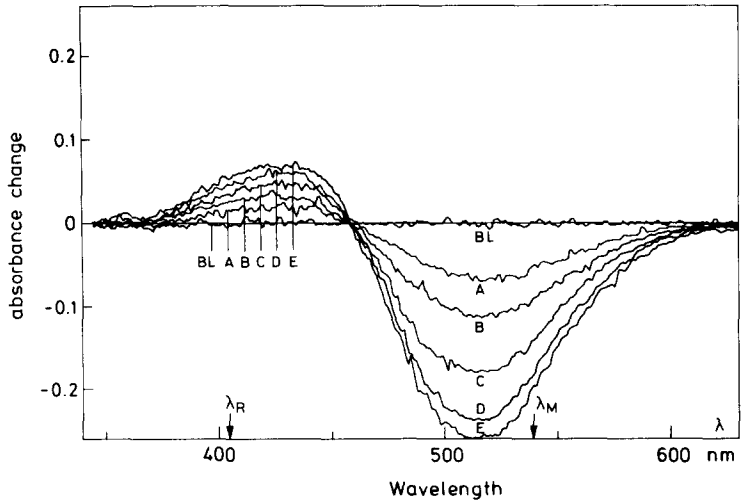

FIGURE 7. Difference spectra of the green-violet-absorbing pigment. The baseline (BL) corresponds to the violet-adapted (405 nm) state. The rhabdom was exposed to light of wavelength 538 nm for different times. *A*: 10 s; *B*: 20 s; *C*: 45 s; *D*: 90 s. Curve *E* was recorded after green exposure of 3 min and represents a saturated state.

unfixed retinas, however, it was not possible to illuminate the rhabdoms end-on because the sliced tissue became deformed. Instead, a slit was projected on the specimen plane and superimposed on an ommatidium suspended horizontally in the Ringer solution. Some of the measurements were also done through squashed retinas. The absorbance change amplitude was very small (change in optical density <0.02) and it was necessary to average at least 20 scans to obtain readable data. Fig. 8 shows the average difference spectrum obtained from these 20 preparations and, for comparison, the average difference spectrum from fixed retinae whose rhabdoms were measured end-on. The curve for the fixed preparations is the average of 32 scans. Qualitatively, the fixed and unfixed preparations do not show any significant difference; there is a slight indication of a shift to longer wavelengths of the

positive peak and of the isosbestic point after fixation, but in view of the noise level in the measurements without fixation, it is difficult to be certain that these changes are significant.

Photoequilibrium Spectrum

To choose parameters suitable for measuring the conversion spectrum, the photoequilibrium spectrum was first measured. This is the ratio of the amplitudes of the difference spectra after different saturating adaptations (Stavenga, 1975*a*; Hillman, 1979). A test wavelength was chosen on the long-wavelength flank of the difference spectrum, where only one of the two photopigment states was expected to absorb. This wavelength (538 nm) was chosen to be close to the cutoff in absorbance of the other stable state in

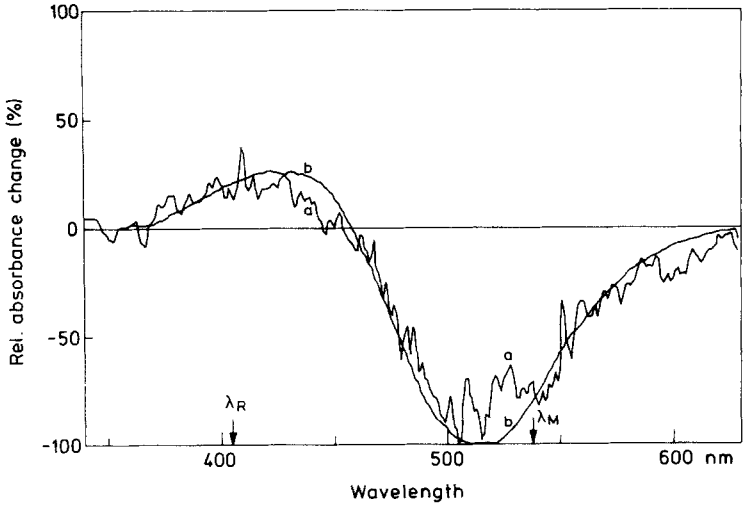

FIGURE 8. Comparison of fixed and unfixed retinas. Difference spectra of the green-violet-absorbing pigment measured through unfixed (*a*) and glutaraldehyde-fixed (*b*) preparations. The adaptation wavelengths were 405 (λ_R) and 538 nm (λ_M). Curve *b* is the average of 32 single rhabdom spectra, measured end-on. Curve *a* is the average spectrum from 20 preparations.

order to maximize the subsequent absorbance change. A baseline absorbance at the test wavelength was first obtained after a saturating adaptation at a longer wavelength (549 nm), which converted the pigment predominantly to the short-wavelength-absorbing (rhodopsin) state. Saturating adaptations at different wavelengths throughout the absorption spectrum were then applied, and the subsequent changes in absorption at the test wavelength measured and plotted as a function of the adapting wavelengths. To average the results from different experiments, each spectrum was normalized at the wavelength of the isosbestic point of the difference spectrum.

The photoequilibrium spectrum obtained in this way (Fig. 9) is, in the present case, a measure of the amount of rhodopsin converted to meta-rhodopsin by the different saturating adaptations. The amplitude is given by

$$Q(\lambda) = [1 - f_R(\lambda)] \cdot [1 + \gamma(\lambda_i)] \quad (1)$$

(Stavenga, 1975*a*; cf. Eq. 11 of the Appendix), where $f_R(\lambda)$ is the fraction of the photopigment as rhodopsin after saturating adaptation at wavelength λ, and $\gamma(\lambda_i)$ is the relative quantum efficiency for photoconversion between the two stable pigment states, measured at the isosbestic wavelength. There are indications that the relative quantum efficiency of invertebrate photopigments is close to unity (Schwemer, 1969; Goldsmith and Bruno, 1973; Tsukahara and Horridge, 1977; Stark and Johnson, 1980), in which case normalization of the photoequilibrium spectrum at the isosbestic point implies that the unity point on the ordinate of Fig. 9 corresponds to 50% conversion to metarhodopsin.

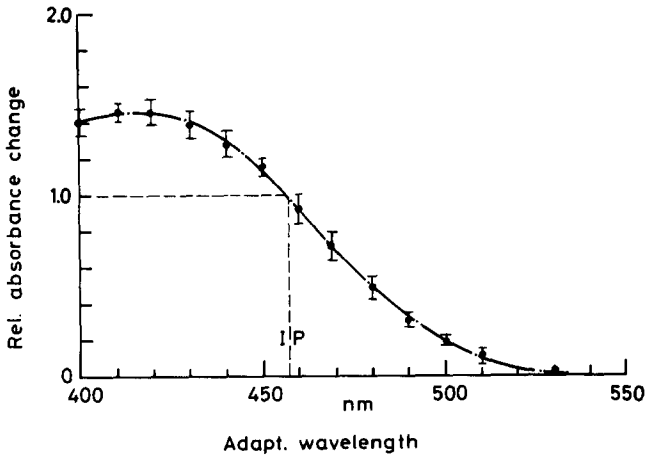

FIGURE 9. Photoequilibrium spectrum of the green-violet-absorbing pigment. The relative absorption change at wavelength 538 nm (outside the overlapping region of the absorption of the two pigment states) was measured after different saturating adaptations (plotted on the abscissa), and with a baseline absorbance after saturating adaptation at 549 nm. The spectra were normalized at the isosbestic point (IP), and are a measure of the relative fraction of the pigment in the rhodopsin or metarhodopsin state after each saturating adaptation (for details, see text). The points are mean values (± SEM) of measurements on rhabdoms from nine retinae.

In principle, the photoequilibrium spectrum can be combined with the difference spectrum to obtain the relative absorption spectra of the two states of the photopigment (Stavenga, 1975*a*), but the resulting spectra are not very accurate (Stavenga, 1976). To do this, furthermore, the photoequilibrium spectrum has to be measured accurately with narrow-bandwidth light. With the apparatus available, this would have been very time-consuming because the monochromator would have had to be adjusted for each illumination and would have produced difficulties because of drift of the preparation. To save time, the adapting lights were obtained from a continuous interference filter with a half-bandwidth of ~15 nm. Hence, although the precision was adequate to establish the maximum and the optimal wavelength

ranges for saturating adaptation (see below), use of the curve for more detailed calculations would have introduced errors.

Conversion Spectra

The photoequilibrium spectrum (Fig. 9) shows that the wavelength that converts the largest fraction of the photopigment to metarhodopsin is at ~410 nm, and that wavelengths longer than 530 nm will convert all the photopigment to rhodopsin. These wavelengths were used for initial adaptation in obtaining the conversion spectra, because optical density changes are then maximal. (In practice, we used a filter with a half-bandwidth of 15

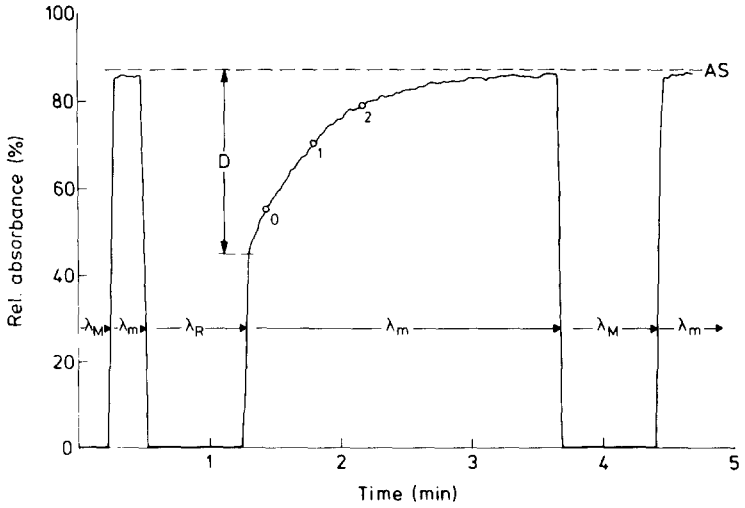

FIGURE 10. Time course of the absorbance change during a photoconversion. The absorbance change during a photoconversion of the green-violet-absorbing pigment was measured at 530 nm (λ_m) after adaptation to 549 (λ_M) and 405 nm (λ_R). The intensity of the measuring beam was sufficiently high to convert the pigment with a time constant of ~1 min. The asymptotic value (AS) was calculated by fitting the curve with an exponential through 0, 1, and 2. AS did not change significantly after several λ_R, λ_M adaptations.

nm centered at 405 nm and a 549-nm cutoff filter.) In brief, the procedure was to measure the optical density change during saturating adaptation at a set of wavelengths after the photopigment had undergone a saturating adaptation at one of the wavelengths for maximum conversion. This is illustrated in Fig. 10, which shows a continuous recording of the optical density change at 530 nm after initial adaptation at 405 nm. During the continuous recording, the optical density change represents the slow photoconversion of the pigment back to rhodopsin. For weak light intensities (where changes in both light scattering and absorption by photostable pigments can be ignored), the rate at which the photoconversion occurs depends only on the intensity of the light and the photosensitivities of the pigment states at the wavelength of the converting light (Hochstein et al., 1978; Minke

and Kirschfeld, 1979). This is not so for the amplitude of the change in optical density at the measuring wavelength. The amplitude will depend on the absorption coefficients of the two pigment states at the measuring wavelength, and also on the change in the fractions of the pigment in the two states when the pigment is converted by the measuring beam. The optical density change is given by the following formula:

$$\Delta D(\lambda) = C_{R,M}(\lambda) = a \cdot [\alpha_R(\lambda) - \alpha_M(\lambda)] \cdot [f_R(\lambda) - f_R(\lambda_{R,M})] \quad (2)$$

(this result is derived in the Appendix; see the discussion leading to Eqs. 14

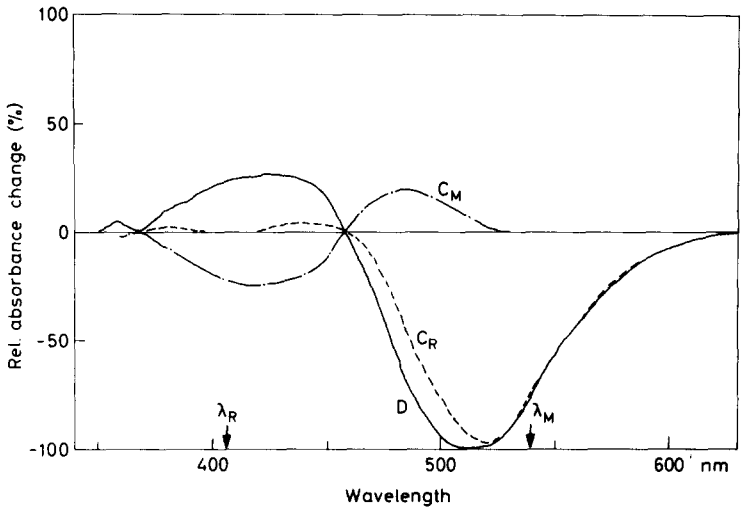

FIGURE 11. Normalized difference spectrum and conversion spectra of the green-violet-absorbing pigment. The difference spectrum was obtained as the absorbance change between spectral scans after saturating adaptation at 405 (λ_R) and 538 nm (λ_M). The conversion spectra were obtained in the same experiments, and measure the optical density change at different wavelengths (cf. Fig. 10) after an initial saturating adaptation at λ_R or λ_M (C_R and C_M, respectively). The difference spectrum is a smoothed average from 32 preparations. The conversion spectra are averaged from 15 determinations and have been interpolated between the 10-nm measuring intervals.

and 21), where a is a factor depending essentially on the amount of photopigment in the rhabdom, α_R and α_M are the absorption coefficients of rhodopsin and metarhodopsin, respectively, f_R is the fraction of the pigment in the rhodopsin state, and $\lambda_{R,M}$ is the initial adapting wavelength that converts the pigment maximally from rhodopsin to metarhodopsin and vice versa. Note that when the initial adaptation is at a long wavelength, which converts all the pigment to rhodopsin, $f_R(\lambda_M)$ is unity. Also, when the measuring wavelength is at the isosbestic point, there is no change in optical density during the adaptation (as found experimentally; see Fig. 11), even though the measurement converts a large fraction of the two states of the pigment.

The conversion spectra thus contain information on the absorption spectra and on the fractions of the pigment in the two states after a saturating adaptation. The detailed procedure for measuring the conversion spectra was the following: (*a*) All the photopigment was first converted to rhodopsin by adaptation using the long-wavelength cutoff filter. (*b*) The initial absorbance at a test wavelength was measured and absorption at this wavelength was followed until equilibrium was reached. The change in absorbance at this test wavelength was calculated. Experimentally, the intensity of the measuring beam was increased from its normal value so that the conversion was complete in a few seconds. (*c*) The photopigment was reconverted to rhodopsin, and photoconversion was then followed at another test wavelength. (*d*) After a set of photoconversions, each starting from rhodopsin, had been obtained, the converse experiment was performed: the pigment was maximally converted to metarhodopsin using the 405-nm filter. Photoconversions were then followed at a series of wavelengths, with reconversion back to metarhodopsin between each test, to give a second set of absorbance changes as a function of wavelength.

Conversion spectra were obtained from a total of 15 preparations, and the pooled results from these experiments are shown in Fig. 11. These curves have been smoothed between the 10-nm measuring intervals. To normalize the conversion spectra with respect to the difference spectrum, it was noted that the sum of the amplitudes of the two conversion spectra must be equal to the difference spectrum (this can be seen by writing out the two equations implicit in Eq. 2 above). Thus, at wavelengths where one of the two conversion spectra was zero, the second was adjusted to have the same amplitude as the difference spectrum (see Fig. 11).

Absorbance Spectra

The saturating difference spectrum and the conversion spectra, as shown in Fig. 11, together with the maximum value of the photoequilibrium spectrum (see Fig. 9), were used to calculate the relative absorption spectra of the rhodopsin and metarhodopsin states of the photopigment. Derivation of the equations used is straightforward, if tedious, and is described in the Appendix (see Eqs. 19, 20, 25, and 26). The only other assumption needed for this calculation was that the relative quantum efficiency (γ) for conversion between the two pigment states is independent of wavelength. The resulting absorption spectra are shown in Fig. 12. The relative absorption spectra can be obtained from the difference spectrum and either of the conversion spectra. For the curves shown in Fig. 12, the calculations were made using the difference spectrum and the conversion spectrum after saturating adaptation to rhodopsin for wavelengths shorter than the isosbestic point and after saturating adaptation to metarhodopsin for wavelengths longer than the isosbestic point. This was done in order to use experimental values of the spectra that were as large as possible (cf. Fig. 11). The curves shown in Fig. 12 were calculated with γ equal to unity. The maxima are at 446 and 505 nm for the rhodopsin and metarhodopsin states, respectively. The ratio of the two amplitudes is 1.72.

The errors in the spectra of Fig. 12 were estimated by repeating the calculations using different values for the difference and conversion spectra, within their 95% confidence limits, and also by varying the value of the maximum of the photoequilibrium spectrum, again within the 95% confidence limits. In this way, the error in the maximum value of the rhodopsin spectrum was estimated to be about ±8 nm, and that in the maximum value of the metarhodopsin spectrum to be about ±5 nm. At the optimum wavelengths, metarhodopsin absorbs more strongly than rhodopsin by a factor of 1.72 ± 0.2.

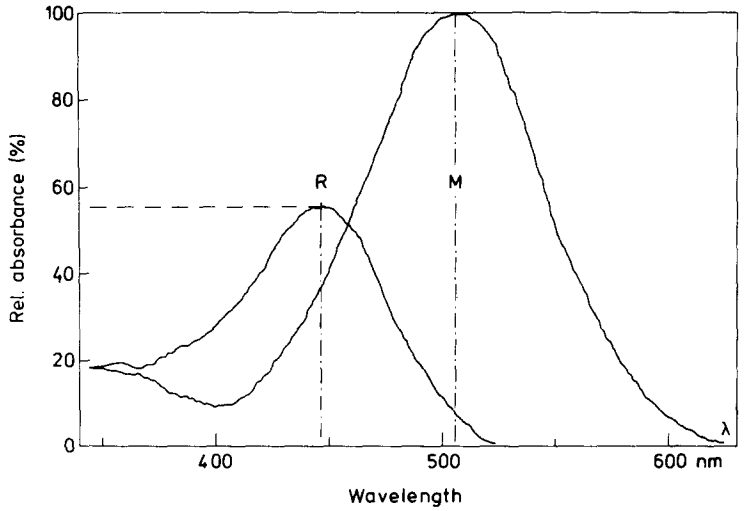

FIGURE 12. Calculated absorbance spectra of the green-violet-absorbing pigment. The relative absorbance profiles of the green-violet-absorbing pigment were calculated from Eqs. 19, 20, 25, and 26 of the Appendix, with the assumption that the relative quantum efficiency is equal to unity. The maximum absorbance of the metarhodopsin was arbitrarily normalized to 100%. For computation, the averaged smoothed difference spectrum and the averaged interpolated conversion spectra were used (see Fig. 11). The accuracy of the peak wavelength for rhodopsin is ±8 nm, and that of the metarhodopsin is ±5 nm.

The relative quantum efficiency is probably close to unity, as for other invertebrate photopigments (Schwemer, 1969; Goldsmith and Bruno, 1973; Tsukahara and Horridge, 1977; Stark and Johnson, 1980). The effect of γ less than unity was calculated for γ equal to 0.9, 0.8, and 0.7. As expected, reduction in the value of γ did not affect the shape of the calculated rhodopsin spectrum (see Appendix), and also produced only small changes in the peak wavelength of the metarhodopsin spectrum, within the experimental error given above. The insensitivity of the calculated metarhodopsin spectrum to reduction in the value of γ results because the major part of this spectrum lies outside the overlapping region of the two absorption spectra. Reduction

in the value of γ, however, significantly affected the ratio of the heights of the calculated absorption spectra. This increased from 1.72 to 1.79, 1.89, and 2.00 for γ equal to 0.9, 0.8, and 0.7, respectively.

A UV-absorbing Pigment

In all the experiments described so far, the wavelengths used for photoconversion were longer than 380 nm, and as has been shown (Fig. 12), only one pigment could be detected. When shorter wavelengths were used, the existence of a second pigment was revealed. The evidence was obtained with the following procedure: (*a*) the preparation was illuminated at 415 nm, to

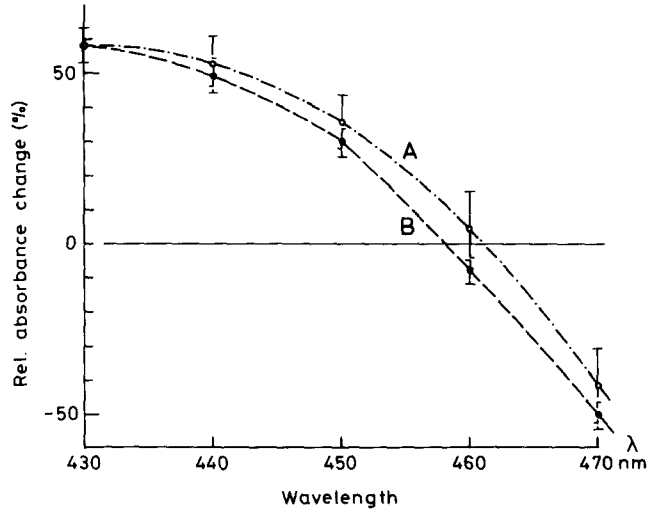

FIGURE 13. Shift of the isosbestic point after UV adaptation. Two difference spectra in the wavelength range including the isosbestic point are compared. *B* shows the absorbance change between violet (415 nm) and green (538 nm) adaptation. When a UV adaptation preceded the violet adaptation, curve *A* was obtained. *A* was normalized to the relative absorbance change of *B* at 430 nm. Each point is the mean ± SEM of 15 observations.

convert any possible UV pigment to the UV-absorbing state; (*b*) the preparation was illuminated at 538 nm, and a spectral scan was made (1); (*c*) the preparation was illuminated at 415 nm and a second spectral scan made (2); the first difference spectrum was obtained as the difference between 1 and 2; (*d*) the preparation was then illuminated with UV light at $\lambda < 370$ nm; (*e*) the preparation was illuminated at 538 nm and a spectral scan was made (3); (*f*) the preparation was illuminated at 415 nm and a spectral scan was made (4); the second difference spectrum was measured as the difference between 3 and 4.

It was found that the two difference spectra did not cross the baseline at the same wavelength. For the first difference spectrum, the wavelength was, of course, the isosbestic point of the pigment described previously (see Fig. 7). After illumination with UV light (step *d*), the crossover was shifted by a

small but significant amount toward the red (Fig. 13). This shows that illumination with UV caused an increase in the quantity of pigment absorbing in the blue-violet.

The same shift in the crossover wavelength could be obtained many times in the same preparation by repeating steps *a–f*. This suggested the existence of a second pigment with two stable states, one absorbing in the UV and one absorbing in the blue-violet, and so absorbance measurements in the UV were undertaken. These absorbance changes were measured after UV adaptation at 325 nm and blue-violet adaptation at 448 nm. The latter wavelength was chosen to be as close as possible (with the filters available) to the isosbestic wavelength of the blue-absorbing rhodopsin-metarhodopsin system. In this way, interference from absorbance changes of this system were minimized. The changes in absorbance in the UV produced by illuminating

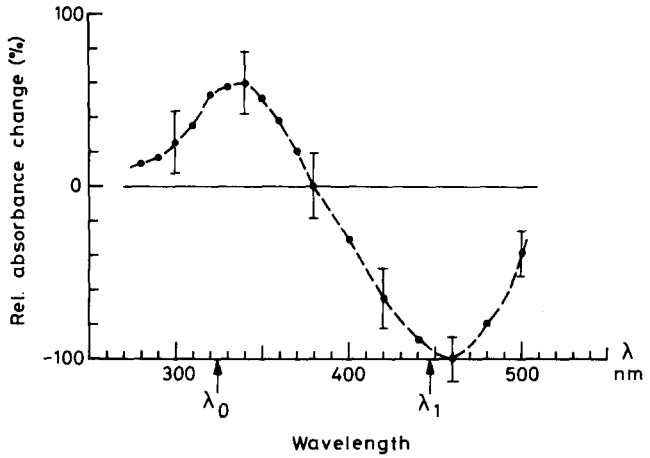

FIGURE 14. Difference spectrum of the UV-violet-absorbing pigment measured through single rhabdoms. The absorbance change was measured between adaptations with light of wavelengths 325 (λ_0) and 448 nm (λ_1). The latter was chosen to be close to the isosbestic point of the green-violet pigment. Individual points are mean ± SEM of 24 observations.

first in the blue-violet and then in the UV were small compared with the total absorbance of the preparation (including scattering). To increase the signal-to-noise ratio, the intensity of the measuring beam and the duration of the measurement were increased so that a significant amount of the pigment would have been photoconverted if a complete scan of the spectrum had been made. Therefore, measurements were made only at intervals of 10 or 20 nm, and between each measurement the pigment was reilluminated with the adapting light. The curve obtained in this way is shown in Fig. 14.

The simplest interpretation of this curve is that there is a pigment that has one state with a maximum absorbance near 340 nm and another state with a maximum in the blue-violet at ~460 nm. The magnitude of the absorbance change at the negative extremum of the curve (460 nm) varied from one preparation to another and was between 2 and 5% of the green maximum

of the difference spectrum of the green-violet pigment (Fig. 11). A more detailed investigation is made difficult by the existence of the green-violet pigment and by fluorescence of the preparation on UV illumination. However, unlike the green-violet pigment, the maximum and minimum of the difference spectrum of the UV-violet pigment are well separated and should correspond fairly closely to the peaks of the absorption spectra.

Transmission of the Dioptric Apparatus

The physiological spectral sensitivity of the intact eye depends not only on the absorbance of the photopigment but also on the transmittance through the dioptric apparatus. The transmittance through the cornea and the crystalline cone of the honeybee drone eye as a function of wavelength is shown in Fig. 15.

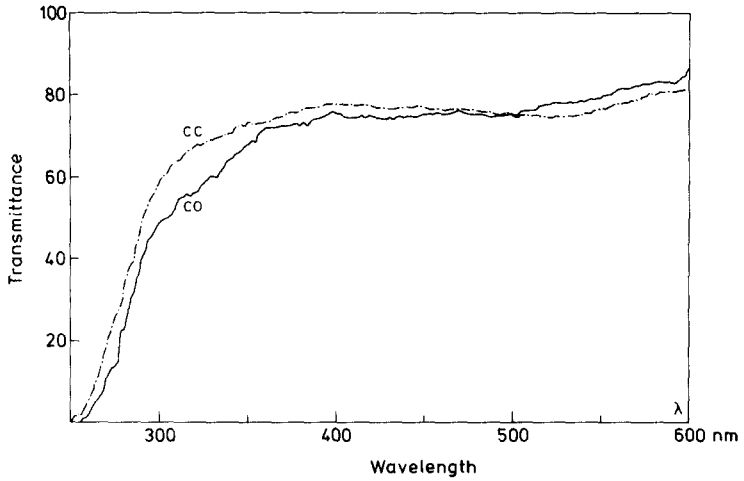

FIGURE 15. Spectral transmittance of the dioptric apparatus. Spectral transmittance of a lenslet in the honeybee drone cornea (CO) and of a crystalline cone (CC). The cornea was cleaned of screening pigments. The transmittance of the crystalline cone, still attached to the ommatidium, was measured side-on.

To measure the transmittance through the center of a corneal facette (CO, Fig. 15), a small piece of cornea was sliced off, cleared of soft tissue, and placed on the stage of the microspectrophotometer. The transmittance of the crystalline cones (CC, Fig. 15) was measured on unfixed preparations of ommatidia with the crystalline cones still attached. The measuring beam was directed side-on. The transmittance is relatively constant from 600 to 350 nm and then drops sharply at shorter wavelengths. The curves are similar in shape to those obtained by Skrzipek and Skrzipek (1974) for the dioptric apparatus of the honeybee worker and also to those measured by Carlson and Philipson (1972) on *Manduca sexta*. Fig. 15 indicates that both the bistable UV-violet and the bistable violet-green pigment of the honeybee drone retina

described above can be expected to have physiological roles in the intact animal.

DISCUSSION

Measurement of the Absorbance Spectra of a Pigment with Two Interconvertible Stable States

The absorbance spectra of the two states of the green-violet pigment were calculated from the difference spectrum, the conversion spectra, and the photoequilibrium spectrum. This calculation was possible because there is a range of wavelengths, toward the red, where the absorbance of one of the pigment states is negligible compared with the absorbance of the other. For any photopigment there are physical grounds for expecting that the absorbance spectrum should fall to zero on the long-wavelength side of its maximum, because in this region photons do not have sufficient energy to cause a transition to the first electronic excited state. Evidence that this is true for visual pigments is given by the absorbance spectra of pigments that bleach, such as vertebrate rhodopsins (Dartnall, 1962).

Hence, in general, if the absorbance spectra of the two states of a pigment have separated maxima and fairly similar profiles, the same condition will be found as for the green-violet pigment in the present work, i.e., there will be a range of wavelengths where only one of the two states has a significant absorbance. From the photoequilibrium spectrum it can be seen that the fraction of pigment converted by light in this range and also around the maximum (410 ± 10 nm) does not depend critically on the wavelength, and this property was used in the present work to maximize the accuracy of the determination of the absorbance spectra. With adaptations in these two ranges, a maximum fraction of pigment is converted to the other state. The difference spectrum used for the calculation of the absorbance profiles was obtained with these adaptation wavelengths, and since the difference spectrum amplitude is then maximal, the signal-to-noise ratio is maximal, too. Without a decrease in accuracy, the adaptation in the two wavelength ranges can be obtained by using interference filters of relatively large bandwidths (15–20 nm). Outside these two wavelength ranges, the bandwidth of the adapting light has to be much smaller and a monochromator must be used, as was necessary for the recording of the conversion spectra. For adaptation in the long-wavelength range, a cutoff filter can also be used. The light flux can thus be chosen relatively high and consequently the adaptation time is short (a few seconds). Only in exceptional cases (cf. Fig. 6) was the preparation sufficiently stable to allow long adaptation times to be used.

The conversion spectrum from the violet and the difference spectrum are identical outside the overlapping area of the absorbance profiles of R and M. This is also the case for the conversion spectrum from the green-yellow and the difference spectrum in the violet wavelength range. Thus, the difference spectrum and conversion spectra from an arbitrary number of preparations

can be measured and averaged separately and then normalized to 100% for the maximum amplitude of the difference spectrum (see Fig. 11).

The Effect of Fixing the Retina with Glutaraldehyde

In the present work the green and the violet states of the predominant pigment were studied mainly in tissues that had been fixed in glutaraldehyde. In unfixed retinae the difference spectra appeared to be the same as those obtained in fixed preparations and the two pigment states also appeared to be thermostable, although it was not possible to exclude the possibility that conversion occurs in the dark, with a time scale of tens of minutes or greater. Hays and Goldsmith (1969) reported that in *Libina* only one pigment state was stable after treatment with glutaraldehyde. It may be that the effect of glutaraldehyde varies from one species to another.

Correlation Between Microspectrophotometry, Anatomy, and Electrophysiology

In the dorsal part of the drone retina each ommatidium contains six large and three much smaller photoreceptor cells (Perrelet and Baumann, 1969). Autrum and Zwehl (1964) and Bertrand et al. (1979) measured the spectral sensitivity of photoreceptor cells in this region with intracellular microelectrodes. Both laboratories found cells with a maximum sensitivity at 450 nm and a spectral sensitivity curve compatible with the 446-nm pigment state reported here. In addition, Autrum and Zwehl (1964) reported cells with a maximum sensitivity at 340 nm, in agreement with the UV-absorbing state of the UV-violet pigment reported here. Bertrand et al. (1979) in their study accepted only those cells whose resting membrane potentials were more negative than −50 mV; conceivably, this selection may have excluded the small cells, which are more prone to damage by the microelectrode. Thus, a simple interpretation would be that the large photoreceptor cells contain the violet-green pigment (the violet-absorbing state being the rhodopsin) and that one or more of the three small photoreceptor cells contain the UV-violet pigment. Wehner (1976) has reported evidence that in worker bees the small photoreceptor cells in the dorsal retina are UV sensitive.

Photoequilibrium of the Violet-Green Pigment In Vivo

The drone does not forage and the aspect of its vision that is presumably most subject to evolutionary pressure is its use in the pursuit of the queen during her nuptial flight. This involves detection of small objects against the background of a blue sky. The spectral irradiance of the blue sky has its maximum near 450 nm (Lythgoe, 1972), the wavelength of maximum sensitivity of the large photoreceptor cells in the dorsal retina of the drone. Illumination with skylight will establish a photoequilibrium between rhodopsin and metarhodopsin. Taking the spectral distribution of skylight with a color temperature of 7,500°K, the photoequilibrum was calculated for the absorbance spectra of rhodopsin and metarhodopsin of Fig. 13. The result obtained was that 72% of the pigment will be present as rhodopsin. Illumination with direct sunlight (5,600°K) will tend to increase this fraction (to 76%). The visual pigment system thus appears to be well adapted, in the

sense that there will be optimal contrast detection for dark objects against a blue background, and that the blue background does not deplete the rhodopsin content to such a low level that changes in incident light can no longer be detected.

appendix

Calculation of the Absorption Spectra

LIST OF SYMBOLS

R, M	rhodopsin, metarhodopsin state of the visual pigment
α_R, α_M	absorption coefficients of R and M
γ_R, γ_M	quantum efficiencies for the photoconversions R to M and M to R
$\gamma = \gamma_M/\gamma_R$	relative quantum efficiency
$f_R(\lambda)$, $f_M(\lambda)$	fraction of pigment as R or M at equilibrium after adaptation with light of wavelength λ
C_P	concentration of pigment molecules (M + R) in the rhabdom
$I(\lambda)$	incident light intensity of wavelength λ
k_R, k_M	rate factors of photochemical reactions
λ_R, λ_M	wavelengths for maximum saturating adaptations of the green-violet photopigment
C_R, C_M	conversion spectrum after adaptation at λ_R or λ_M
D_R, D_M	saturating difference spectra between adaptations at λ_R and λ_M; $D_R = -D_M$
l	length of the rhabdom in the preparation

It is shown here how the relative absorption spectra of the two stable states of the drone photopigment can be obtained from measurements of the difference spectrum, the maximum amplitude of the photoequilibrium spectrum, and the conversion spectra.

In the present work, only changes in absorbance between stable states of the photopigment are considered. It is assumed that the major absorbance changes are due to the presence of a single photopigment with two photointerconvertible states, designated R for rhodopsin, and M for metarhodopsin. If the photoequilibrium between these states can be described as a reversible first-order reaction (Hamdorf, 1979), then at equilibrium after a saturating adaptation with monochromatic light (wavelength λ_a), the fraction of the photopigment in states R and M will be (Stavenga, 1975*a*):

$$f_R(\lambda_a) = \frac{k_M(\lambda_a)}{k_R(\lambda_a) + k_M(\lambda_a)}, \qquad f_M(\lambda_a) = \frac{k_R(\lambda_a)}{k_R(\lambda_a) + k_M(\lambda_a)}, \tag{3}$$

where the rate factors k_R and k_M are:

$$k_R = \alpha_R(\lambda_a)\cdot\gamma_R(\lambda_a)\cdot I(\lambda_a), \qquad k_M(\lambda_a) = \alpha_M(\lambda_a)\cdot\gamma_M(\lambda_a)\cdot I(\lambda_a). \tag{4}$$

(More strictly, these rate factors should be taken as averages over the wavelength-intensity range of the light intensity I, but it is assumed that the incident light is sufficiently monochromatic to avoid this complication.) After a saturating adaptation, the fractional concentrations of the photopigment in states R or M will be uniform along the rhabdom. The optical density of the rhabdom at wavelength λ will then be (cf. Hamdorf, 1979),

$$\mathrm{OD} = (\log e)\cdot\int_0^l \eta(\lambda, x)\cdot\{[f_R(\lambda_a)\cdot\alpha_R(\lambda) + f_M(\lambda_a)\cdot\alpha_M(\lambda)]C_P(x) + S(\lambda, x)\}\cdot dx, \tag{5}$$

where η is a factor accounting for the waveguide properties of the rhabdom, C_P is the photopigment concentration, and S is a factor that includes all light-scattering phenomena, together with absorption by any photostable pigments.

For large rhabdoms, such as those of the drone, it can be shown that wavelength cutoff effects are not expected to be present, and thus η is independent of λ. The scattering term S is strongly dependent on wavelength (see Fig. 5). However, it must have been constant, at least within the time course of an individual experiment, otherwise it would not have been possible to obtain repeatable measurements of an isosbestic point from difference spectra (cf. below). Eq. 5 then reduces to

$$\mathrm{OD} = a \cdot [f_R(\lambda_a) \cdot \alpha_R(\lambda) + f_M(\lambda_a) \cdot \alpha_M(\lambda)] + b(\lambda), \tag{6}$$

where

$$a = (\log e) \cdot \int_0^l \eta(x) \cdot C_P(x) \cdot dx \tag{7}$$

is a constant independent of wavelength, and

$$b(\lambda) = (\log e) \cdot \int_0^l \eta(x) \cdot S(x, \lambda) \cdot dx \tag{8}$$

is a term that depends on measuring wavelength λ, but is considered to be otherwise constant.

Difference Spectra

Measurements of difference spectra are obtained from differences between the amplitudes of spectral scans after different saturating adaptations. During these scans, the fraction of the pigment in each state remains constant (or is assumed to change only negligibly), and the parameters a and b, as defined above, will also be constant because they are independent of adapting wavelength. From Eq. 6, since $f_R(\lambda) = 1 - f_M(\lambda)$, the difference spectra are then given by

$$D(\lambda) = a \cdot [\alpha_R(\lambda) - \alpha_M(\lambda)] \cdot [f_R(\lambda_a) - f_R(\lambda_b)], \tag{9}$$

where λ_a and λ_b are the adapting wavelengths, and the optical density scan after adaptation at λ_b has been taken as baseline. It is clear that difference spectra do not allow separation of α_R and α_M. However, as shown by Stavenga (1975*a*), a comparison of the amplitudes of the difference spectra provides information on the relative occupancy of the two states of the photopigment after different saturating adaptations and also, indirectly, using Eqs. 3 and 4, on the relative absorption spectra.

From Eq. 9, the relative amplitudes of difference spectra between adaptations at λ_a and λ_b and at λ_a and λ_r is

$$\frac{D(\lambda_a/\lambda_b)}{D(\lambda_a/\lambda_r)} = \frac{f_R(\lambda_a) - f_R(\lambda_b)}{f_R(\lambda_a) - f_R(\lambda_r)}. \tag{10}$$

However, it can be expected that for the two states of the photopigment, there will be a region on the long-wavelength side of the absorption spectra, where only one state of the pigment absorbs significantly (see Discussion). For the drone photopigment, this will be due to absorption by the M state only, and if λ_a is chosen to be in this region, $f_R(\lambda_a) = 1$. Additionally, if λ_r is chosen to be the wavelength at the isosbestic point, λ_i where $\alpha_R(\lambda_i) = \alpha_M(\lambda_i)$, Eqs. 3 and 4 imply that $f_R(\lambda_i) = \gamma(\lambda_i)/[1 + \gamma(\lambda_i)]$, where γ is the relative quantum efficiency. Eq. 10 then becomes (cf. Stavenga,

1975*a*), with $\lambda = \lambda_b$ as independent variable,

$$Q(\lambda) = \frac{D(\lambda_a/\lambda)}{D(\lambda_a/\lambda_i)} = [1 - f_R(\lambda)]\cdot[1 + \gamma(\lambda_i)], \tag{11}$$

which in the present nomenclature is the photoequilibrium spectrum (Hillman, 1979), and is a measure of the fraction of the pigment in state R or M in equilibrium at wavelength λ. The results of measurements of this spectrum for the principal photopigment of the drone are shown in Fig. 9.

Conversion Spectrum

Combination of Eqs. 9 and 11, using Eqs. 3 and 4 for the fractional occupancy of R and M at equilibrium, enables us to obtain the relative absorption spectra of the two states (Stavenga, 1975*a*). However, the results are not very accurate (Stavenga, 1976), and thus, to overcome this problem at least partially, a new spectrum, the conversion spectrum, was measured. This spectrum is a measure of the change in optical density during adaptation at an independent wavelength (λ) after saturating adaptation at a given wavelength λ_a. Since adaptation at λ after adaptation at λ_a involves both a change in photopigment states and different absorption coefficients, the spectrum measures a mixing of the difference spectrum and the photoequilibrium spectrum. This might seem to be disadvantageous. However, this spectrum is not only simple to measure but can be measured more accurately than the difference spectra because the initial adapting wavelengths can be chosen to give maximum responses.

The conversion spectrum will be maximal when the initial adapting wavelengths convert the maximum of the photopigment from R to M or from M to R. The starting point is therefore the photoequilibrium spectrum (see Fig. 9). These wavelengths are designated λ_R and λ_M, respectively. If the photopigment is first adapted at λ_R, the initial optical density at measuring wavelength λ will be

$$\mathrm{OD} = a\cdot[f_R(\lambda_R)\cdot\alpha_R(\lambda) + f_M(\lambda_R)\cdot\alpha_M(\lambda)] + b(\lambda), \tag{12}$$

and the final optical density, after adaptation at λ, will be

$$\mathrm{OD} = a\cdot[f_R(\lambda)\cdot\alpha_R(\lambda) + f_M(\lambda)\cdot\alpha_M(\lambda)] + b(\lambda). \tag{13}$$

The conversion spectrum is the difference between Eqs. 13 and 12. Whence, remembering that $f_R(\lambda) = 1 - f_M(\lambda)$,

$$C_R(\lambda) = a\cdot[\alpha_R(\lambda) - \alpha_M(\lambda)]\cdot[f_R(\lambda) - f_R(\lambda_R)], \tag{14}$$

with, from Eqs. 3, 4, and 11,

$$f_R(\lambda) = \frac{\alpha_M(\lambda)\cdot\gamma(\lambda)}{\alpha_R(\lambda) + \alpha_M(\lambda)\cdot\gamma(\lambda)}, \qquad f_R(\lambda_R) = 1 - \frac{Q(\lambda_R)}{1 + \gamma(\lambda_i)}. \tag{15}$$

At the same time, the difference spectrum of maximum amplitude, between adaptation at λ_R and λ_M, with the spectral scan after adaptation at λ_R as baseline, is (see Eq. 9)

$$D_R(\lambda) = a\cdot[\alpha_R(\lambda) - \alpha_M(\lambda)]\cdot[1 - f_R(\lambda_R)], \tag{16}$$

because $f_R(\lambda_M) = 1$, since adaptation at long wavelengths converts all the photopigment to rhodopsin.

Relative Absorption Spectra

The relative absorption spectra are obtained from the conversion spectrum, the difference

spectrum, and the maximum amplitude of the photoequilibrium spectrum, using the following equations, given by combining Eqs. 14 and 16 and using Eq. 15:

$$\alpha_R(\lambda) = \left(\frac{1}{a}\right)\cdot\gamma(\lambda)\cdot[1 + \gamma(\lambda_i)]\cdot D_R(\lambda) \cdot \frac{D_R(\lambda) - C_R(\lambda)}{\{[1 + \gamma(\lambda)]\cdot Q(\lambda_R) - [1 + \gamma(\lambda_i)]\}\cdot D_R(\lambda) - [1 + \gamma(\lambda)]\cdot Q(\lambda_R)\cdot C_R(\lambda)}, \tag{17}$$

$$\alpha_M(\lambda) = \left(\frac{1}{a}\right)\cdot[1 + \gamma(\lambda_i)]\cdot D_R(\lambda) \cdot \frac{C_R(\lambda) + \{[1 + \gamma(\lambda_i)]/Q(\lambda_R) - 1\}\cdot D_R(\lambda)}{\{[1 + \gamma(\lambda)]\cdot Q(\lambda_R) - [1 + \gamma(\lambda_i)]\}\cdot D_R(\lambda) - [1 + \gamma(\lambda)]\cdot Q(\lambda_R)\cdot C_R(\lambda)}. \tag{18}$$

In order to apply Eqs. 17 and 18, a further assumption is necessary: that the relative quantum efficiency is independent of wavelength, i.e., that $\gamma(\lambda) = \gamma(\lambda_i) = \gamma$. In this case, these equations reduce to

$$\alpha_R(\lambda) = \left(\frac{1}{a}\right)\cdot\gamma\cdot D_R(\lambda)\,\frac{D_R(\lambda) - C_R(\lambda)}{[Q(\lambda_R) - 1]\cdot D_R(\lambda) - Q(\lambda_R)\cdot C_R(\lambda)}, \tag{19}$$

$$\alpha_M(\lambda) = \left(\frac{1}{a}\right)\cdot D_R(\lambda)\,\frac{C_R(\lambda) + [1 + \gamma - Q(\lambda_R)]\cdot D_R(\lambda)/Q(\lambda_R)}{[Q(\lambda_R) - 1]\cdot D_R(\lambda) - Q(\lambda_R)\cdot C_R(\lambda)}. \tag{20}$$

Eqs. 19 and 20 refer to the situation where measurements are made after saturating adaptation at the wavelength that converts a maximum of the photopigment from state R to state M. If measurements are made after adaptation at the wavelength (λ_M), which converts the maximum of the pigment in the opposite direction, the resulting equations for α_R and α_M are somewhat simpler, since in this case, the conversion is complete. That is, $f_R(\lambda_M) = 1$; the conversion spectrum is given by

$$C_M(\lambda) = a\cdot[\alpha_R(\lambda) - \alpha_M(\lambda)]\cdot[f_R(\lambda) - 1], \tag{21}$$

and the maximum difference spectrum, with adaptation at λ_M as baseline, is

$$D_M(\lambda) = a\cdot[\alpha_R(\lambda) - \alpha_M(\lambda)]\cdot[f_R(\lambda_R) - 1]. \tag{22}$$

The solution of Eqs. 21 and 22 for the absorption coefficients, using Eq. 15, is

$$\alpha_R(\lambda) = \left(\frac{1}{a}\right)\cdot\gamma(\lambda)\cdot D_M(\lambda)\,\frac{C_M(\lambda)}{D_M(\lambda) - Q(\lambda_R)\cdot C_M(\lambda)\cdot[1 + \gamma(\lambda)]/[1 + \gamma(\lambda_i)]}, \tag{23}$$

$$\alpha_M(\lambda) = \left(\frac{1}{a}\right)\cdot D_M(\lambda)\,\frac{[1 + \gamma(\lambda_i)]\cdot D_M(\lambda)/Q(\lambda_R) - C_M(\lambda)}{D_M(\lambda) - Q(\lambda_R)\cdot C_M(\lambda)\cdot[1 + \gamma(\lambda)]/[1 + \gamma(\lambda_i)]}, \tag{24}$$

which reduce, on assuming that $\gamma(\lambda) = \gamma(\lambda_i) = \gamma$, to

$$\alpha_R(\lambda) = \left(\frac{1}{a}\right)\cdot\gamma\cdot D_M(\lambda)\,\frac{C_M(\lambda)}{D_M(\lambda) - Q(\lambda_R)\cdot C_M(\lambda)}, \tag{25}$$

$$\alpha_M(\lambda) = \left(\frac{1}{a}\right)\cdot D_M(\lambda)\,\frac{(1 + \gamma)\cdot D_M(\lambda)/Q(\lambda_R) - C_M(\lambda)}{D_M(\lambda) - Q(\lambda_R)\cdot C_M(\lambda)}. \tag{26}$$

It is noted here that the form of Eqs. 19, 20, 25, and 26 indicates that calculation of the relative absorption spectra by the present method involves using only one value from the photoequilibrium spectrum, its maximum [$Q(\lambda_R)$], which can be measured relatively

accurately from a number of experiments, together with measurement of the difference spectrum and the conversion spectra. With appropriate normalization procedures (see text), the relative absorption spectra can therefore be obtained from a large number of spectra from different preparations. On the other hand, although it is also clear that, after normalization, the resulting spectrum for the R state is independent of the value of the relative quantum efficiency (γ), the absorption spectrum for the M state depends on the value taken for γ. It is thus not possible to remove the difficulty, which was also present in the work of Stavenga (1975*a*), that the shape of at least one of the absorption spectra cannot be determined precisely.

Prof. F. Baumann and Drs. J. A. Coles and C. R. Bader provided valuable discussion, constant encouragement, and helpful criticism of early versions of the manuscript. Mr. S. Poitry made useful comments concerning the Appendix. Prof. M. Golay kindly gave permission for use of laboratory and other facilities at the Geneva Observatory. The final version of the manuscript was carefully typed by Ms. N. Collet, and photographic work was by F. Pillonel.

This work was supported by grants from the Swiss National Science Foundation. During part of the work described here, G.J.J. was a Fellow of the European Scientific Exchange Programme.

Received for publication 10 July 1982 and in revised form 3 January 1983.

REFERENCES

Autrum, H., and V. Zwehl. 1964. Die spektrale Empfindlichkeit einzelner Sehzellen des Bienenauges. *Z. Vgl. Physiol.* 48:357–384.

Bader, C. R., F. Baumann, and D. Bertrand. 1976. Role of intracellular calcium and sodium in light adaptation in the retina of the honeybee drone (*Apis mellifera* L.). *J. Gen. Physiol.* 67:475–491.

Bader, C., F. Baumann, D. Bertrand, J. Carreras, and G. Fuortes. 1982. Diffuse and local effects of light adaptation in photoreceptors of the honeybee drone. *Vision Res.* 22:311–317.

Baumann, F. 1975. Electrophysiological properties of the honeybee retina. *In* The Compound Eye and Vision in Insects. G. A. Horridge, editor. Clarendon Press, Oxford. 53–74.

Bertrand, D., G. Fuortes, and R. B. Muri. 1979. Pigment transformation and electrical responses in retinula cells of drone (*Apis mellifera*). *J. Physiol. (Lond.).* 296:431–441.

Carlson, S. D., and B. Philipson. 1972. Microspectrophotometry of the dioptric apparatus and compound rhabdom of the moth (*Manduca sexta*). *J. Insect Physiol.* 18:1721–1731.

Dartnall, H. J. A. 1962. The photobiology of visual processes. *In* The Eye. H. Davson, editor. Academic Press, Inc., New York. 2:321–533.

Goldsmith, T. H. 1972. The natural history of invertebrate visual pigments. *In* Handbook of Sensory Physiology. H. J. A. Dartnall, editor. Springer-Verlag, Berlin. VII/1:685–719.

Goldsmith, T. H., and M. S. Bruno. 1973. Behaviour of rhodopsin and metarhodopsin in isolated rhabdoms of crabs and lobster. *In* Biochemistry and Physiology of Visual Pigments. H. Langer, editor. Springer-Verlag, Berlin. 147–153.

Hamdorf, K. 1979. The physiology of invertebrate visual pigment. *In* Handbook of Sensory Physiology. H. Autrum, editor. Springer-Verlag, Berlin. VII/6A:145–224.

Hamdorf, K., J. Schwemer, and U. Tauber. 1968. Der Sehfarbstoff, die Absorption der Rezeptoren und die spektrale Empfindlichkeit der Retina von *Eledone moschata*. *Z. Vgl. Physiol.* 60:375–415.

Hays, D., and T. H. Goldsmith. 1969. Microspectrophotometry of the visual pigment of the spider crab Libina emarginata. *Z. Vgl. Physiol.* 65:218–232.

Hillman, P. 1979. Bistable and sensitizing pigments in vision. *Biophys. Struct. Mechanism.* 5:111–112.

Hochstein, S., B. Minke, and P. Hillman. 1973. Antagonistic components of the late receptor potential in the barnacle photoreceptor arising from different stages of the pigment process. *J. Gen. Physiol.* 62:105–128.

Hochstein, S., B. Minke, P. Hillman, and B. W. Knight. 1978. The kinetics of visual pigment systems. I. Mathematical analysis. *Biol. Cybernet.* 30:23–32.

Lythgoe, J. N. 1972. The adaptation of visual pigments to the photic environment. *In* Handbook of Sensory Physiology. H. J. A. Dartnall, editor. Springer-Verlag, Berlin. VII/1:566–603.

Minke, B., and K. Kirschfeld. 1979. The contribution of a sensitizing pigment to the photosensitivity spectra of fly rhodopsin and metarhodopsin. *J. Gen. Physiol.* 73:517–540.

Muri, R. B. 1979. Microspectrophotometrie visible et UV des rhabdomes isolés de la rétine du faux-bourdon (*Apis mellifera* ♂). Thesis, University of Geneva.

Perrelet, A. 1970. The fine structure of the retina of the honeybee drone. *Z. Zellforsch. Mikrosk. Anat.* 108:530–562.

Perrelet, A., and F. Baumann. 1969. Presence of three small retinula cells in the ommatidium of the honeybee drone eye. *J. Microsc. (Paris).* 8:497–502.

Schwemer, J. 1969. Der Sehfahrbstoff von *Eladone moschata* und seine Umsetzungen in der lebenden Netzhaut. *Z. Vgl. Physiol.* 62:121–152.

Shaw, S. R. 1969. Interreceptor coupling in ommatidia of drone honeybee and locust compound eyes. *Vision Res.* 9:999–1029.

Skrzipek, K.-H., and H. Skrzipek. 1974. Die spektrale Transmission und die optische Aktivitaet des dioptrischen Appartes der Honigbiene (*Apis mellifica*). *Experientia.* 30:314–315.

Stark, W. S., and M. A. Johnson. 1980. Microspectrophotometry of *Drosophila* visual pigments: determinations of conversion efficiency in R1-6 receptors. *J. Comp. Physiol.* 140:275–286.

Stavenga, D. G. 1975*a*. Derivation of photochrome absorption spectra from absorbance difference measurements. *Photochem. Photobiol.* 21:105–110.

Stavenga, D. G. 1975*b*. Waveguide modes and refractive index in photoreceptors of invertebrates. *Vision Res.* 15:323–330.

Stavenga, D. G. 1976. Fly visual pigments. Difference in visual pigments of blowfly and dronefly peripheral retinula cells. *J. Comp. Physiol.* 111:137–152.

Tsukahara, Y., and G. A. Horridge. 1977. Visual pigment spectra from sensitivity measurements after chromatic adaptation of single dronefly retinula cells. *J. Comp. Physiol.* 114:233–251.

Varela, F. G., and W. Wiitanen. 1970. The optics of the compound eye of the honeybee (*Apis mellifera*). *J. Gen. Physiol.* 55:336–358.

Wehner, R. 1976. Structure and function of the peripheral visual pathway in hymenopterans. *In* Neural Principles in Vision. F. Zettler and R. Weiler, editors. Springer-Verlag, Berlin. 280–333.